QGRAPH-BOUNDED Q-LEARNING: STABILIZING MODEL-FREE OFF-POLICY DEEP RL

Anonymous authors
Paper under double-blind review

ABSTRACT

In state of the art model-free off-policy deep reinforcement learning (RL), a replay memory is used to store past experience and derive all network updates. Even if both state and action spaces are continuous, the replay memory only holds a finite number of transitions. We represent these transitions in a *data graph* and link its structure to soft divergence. By selecting a subgraph with a favorable structure, we construct a simple Markov Decision Process (MDP) for which exact Q-values can be computed efficiently as more data comes in – resulting in a QGRAPH. We show that the Q-value for each transition in the simplified MDP is a lower bound of the Q-value for the same transition in the original continuous Q-learning problem. By using these lower bounds in TD learning, our method is less prone to soft divergence and exhibits increased sample efficiency while being more robust to hyperparameters. QGRAPHs also retain information from transitions that have already been overwritten in the replay memory, which can decrease the algorithm's sensitivity to the replay memory capacity.

1 INTRODUCTION

With the wide-spread success of deep neural networks, also deep reinforcement learning (RL) has enabled rapid improvements in many domains including computer games (Silver et al., 2017) and simulated continuous control tasks (Mnih et al., 2016). Particularly in areas where correct environment models are hard to obtain, such as robotic manipulation, model-free approaches have the potential to outperform model-based solutions (Fazeli et al., 2017; Levine et al., 2016) – as long as enough training data is available or can be generated.

Although efforts in the research community on building an understanding of deep RL for simple examples seem to be rising (Mania et al., 2018), deep reinforcement learning remains under-investigated from a theoretical point of view. Many algorithms use function approximation, off-policy learning and bootstrapping together – which has even been called *deadly triad* by Sutton & Barto (2018) because this is a very unstable combination of techniques. Although Q-learning is known to have convergence issues even with linear function approximation (Baird, 1995), deep Q-learning descendants like DQN and DDPG often excel empirically (Van Hasselt et al., 2018). At the same time their performance can be unreliable and hard to reproduce (Henderson et al., 2018).

To add to the community's understanding of when deep Q-learning diverges, we propose a graph-perspective on the replay memory which allows to analyze its structure. We show on educational examples which types of structures are linked to divergence, derive our method from these cases and show that it prevents many cases of soft divergence and thereby helps to stabilize model-free off-policy deep reinforcement learning.

2 PRELIMINARIES

We consider a standard reinforcement learning setup where an agent interacts in discrete time steps $t = 1, \ldots, T$ with an environment that is modeled as a Markov decision process (MDP) with a state space $\mathcal{S}$, action space $\mathcal{A}$, an initial state distribution $p(s_1)$, transition dynamics $p(s_{t+1}|s_t, a_t)$ and a reward function $r(s_t, a_t)$. In the following, we will assume deterministic transition dynamics.

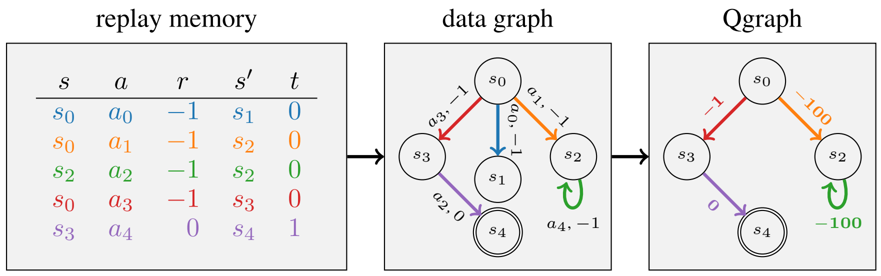

s	a	r	s'	t
s_0	a_0	-1	s_1	0
s_0	a_1	-1	s_2	0
s_2	a_2	-1	s_2	0
s_0	a_3	-1	s_3	0
s_3	a_4	0	s_4	1

Figure 1: We take a graph perspective on past experience (middle) and extract a subgraph (right) such that its structure allows to compute exact Q-values using Q-iteration the resulting simplified and finite MDP. Its Q-values represent lower bounds to the Q-values in the actual continuous MDP.

At each time t, the agent can observe its state s_t and take an action a_t which determines the next state s_{t+1} and an associated reward r_t. A policy is a function π that maps from states to actions. The sum over future expected rewards when following policy π is called return: $R^\pi = \sum_{i=t}^{T} \gamma^{i-t} r_i$, where γ is the so-called discount factor. For $\gamma < 1$ and a constant reward r for infinite trajectories, the return forms a geometric series and converges to $\frac{r}{1-\gamma}$. This also means, that if the reward function is bounded by R_{min} and R_{max}, the smallest and largest possible Q-value can be computed as

$$\left[\text{min}\left(R_{\text{min}}, \frac{R_{\text{min}}}{1-\gamma}\right), \max\left(R_{\text{max}}, \frac{R_{\text{max}}}{1-\gamma}\right)\right] \tag{1}$$

respectively (Lee & Kim, 2015). The min/max operations ensure that also cases when terminal states are reached are covered.

Analogously, if the reward only depends on the current state and the agent stays in a state s forever, because action $a = \pi(s)$ does not lead to a change in states, then $\mathcal{Q}(s,a) = \frac{r}{1-\gamma}$. This transfers to larger loops, e.g. if transitions (s_1, a_1, r_1, s_2) to (s_n, a_n, r_n, s_1) are known to be induced by a policy π,

$$Q(s_1, \pi(s_1)) = \underbrace{r_1 + \gamma r_2 + ... + \gamma^{n-1} r_n}_{r_L} + \gamma^n r_1 + \gamma^{n+1} r_2 + ... = r_L \sum_t^\infty (\gamma^n)^t = \frac{r_L}{1-\gamma^n} \tag{2}$$

The expected future return for executing an arbitrary action a_t and then following the policy is called $Q^\pi(s_t, a_t) = \mathbb{E}\left[r_t + \gamma \cdot R^\pi_{t+1}\right]$. The agent's goal is to find the optimal policy π^* such that the expected future return is maximized from any state. This can be achieved by finding (a good approximation to) the Q-function and then choosing the action with highest Q-value in each state.

One popular way to learn a Q-function is temporal difference (TD) learning. Given a transition (s, a, r, s'), the next Q-value $Q'(s,a)$ is computed based on the current estimate for state s',

$$\mathcal{Q}'(s,a) = r + \begin{cases} 0, & \text{if } s' \text{ is terminal} \\ \gamma \cdot \mathcal{Q}(s', \pi(s')), & \text{else} \end{cases} \tag{3}$$

Such a process with updates that are based on the current estimates of the function to be approximated is called *bootstrapping*. Note that bootstrapping is actually only applied in the case of non-terminal states (i.e. in the second line of the equation). We refer to states that do not require bootstrapping to estimate a Q-value as *anchors*.

In small settings with finitely many states and actions, $\mathcal{Q}$ can be represented as a table – this form of Q-learning is referred to as *tabular*. The policy in tabular Q-learning can be read of the table as $\pi(s) = \arg\max_a \mathcal{Q}(s,a)$. In continuous state or action spaces, Eq. (3) can be used with function approximation.

3 Related Work

One of the most popular function approximators for Q-functions are neural networks: In deep Q networks (DQN), a single network is trained to take states as an input and output one Q-value for each possible action (Mnih et al., 2015). For continuous actions, an actor-critic architecture can be used: the policy is approximated by one network (the so-called actor), while a second network estimates the Q-value for a state-action pair (the critic). In deep deterministic policy gradients (DDPG), the critic's estimates are then used as a training signal for the actor network (Lillicrap et al., 2015).

Both DDPG and DQN are model-free algorithms, i.e. do not assume nor learn a model of the environment (including dynamics and other objects in the environment). Furthermore, they use off-policy data, i.e. they store past experience in a replay memory and update their networks based on this experience, even if the policy π has changed since the data was collected. It is insightful to note that this replay memory only contains a finite number of transitions (s, a, r, s', t) that all networks are updated from, even for continuous state-action spaces.

The original reasoning behind replay memories and experience replay was to break dependencies between transitions (Mnih et al., 2015), which is important for most function approximation schemes. We will therefore keep the principle of random selection of data for our learning process, but at the same time we will make use of additional information that a graph perspective can provide and would be lost otherwise. Prior work has incorporated trajectory-centric perspectives already: Monte Carlo updates for example do not estimate Q-values based on single transitions as in Eq. (3) but on empirical returns for full episodes. Many intermediate algorithms exist, mixing TD-learning and Monte Carlo approaches, (e.g. Amiranashvili et al. (2018); Munos et al. (2016)) but often the resulting gradients on the Q-function suffer from large variance (Doerr et al., 2019). Trajectories have also been combined to graph structures, for instance to guide exploration (Shkolnik & Tedrake, 2009), to allow for planning (Farquhar et al., 2018) or to re-visit previously discovered states (Dong et al., 2019).

Despite its success in many applications, model-free off-policy deep reinforcement learning can be rather unstable: On the one hand, many algorithms are very sensitive to hyperparameters and even subtle differences in their implementation (Henderson et al., 2018), making it hard to provide sensible empirical comparisons. On the other hand, the theoretical underpinning is quite weak: Reinforcement learning with (even linear) function approximation has already been known to be instable for more than 20 years (Baird, 1995). Since DQN and DDPG combine (highly non-linear) function approximation with bootstrapping and off-policy learning, these algorithms are in a category of methods that Sutton & Barto (2018) call *deadly triad* because it is even more prone to divergence. Other types of off-policy reinforcement learning are much better understood and proven to converge under certain conditions, e.g. for prediction in finite MDPs with non-linear function approximation as in (Maei et al., 2009) or control under the assumption of a stationary policy (Maei et al., 2010). Also simplified MDPs have been examined for reinforcement learning, for instance to combine model-based and model-free methods as in Seijen et al. (2011).

Since empirical success seems to be on the side of DQN and DDPG though, there has been an increasing number of works on simpler reinforcement learning on the one hand (Mania et al., 2018) and analyses of small examples to build an understanding of why this often works so well. Van Hasselt et al. (2018) for instance show that *unbounded* divergence, which would cause floating point NaNs, as expected for the deadly triad, barely happens in deep Q-learning. Instead, typically only *soft* divergence, causing Q-values beyond the realizable range, is observed. Nonetheless, all variants of divergence not just lead to instable Q-estimates but also prolong the learning phase – which is particularly painful for areas with high costs associated to new data samples such as robotics. Our method, QGRAPH-bounded Q-learning, analyzes cases of soft divergence and prevents many of them by establishing and using Qgraph-based lower bounds for Q-values.

4 EDUCATIONAL EXAMPLES

Let's assume a continuous state-action space, but the replay memory only contains up to four transitions and three states (one of which is terminal). Figure 2 illustrates this as a graph, where each node is a state and each edge represents a transition. Under the assumption that it is possible for an agent to have discovered any subset of transitions, $2^4 = 16$ cases emerge from this setting (one of which is empty and therefore ignored).

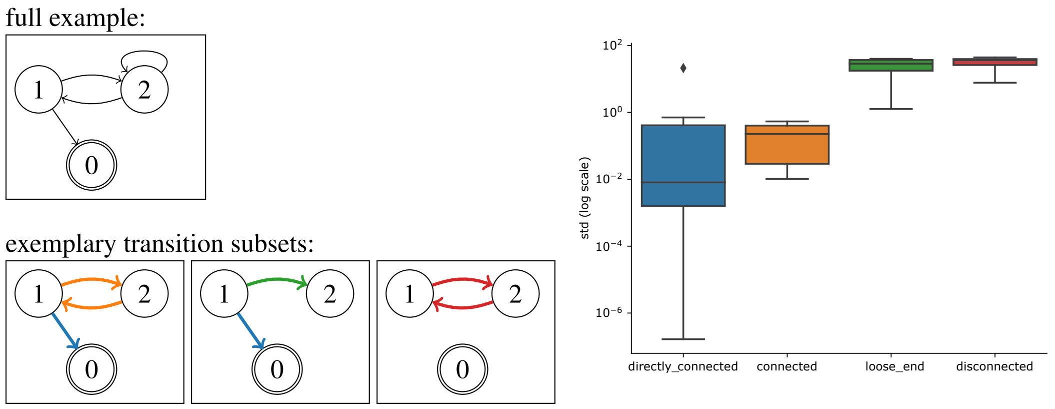

Figure 2: Illustration of the educational example with four transitions and three states (where state 0 is terminal). We characterize transition subsets based on their graph structure: (in-)directly connected to a terminal state (blue, orange); loose ends (green) and disconnected but infinite paths (red). The right plot illustrates the standard deviation over predicted Q-values for each type of transition.

We have trained a DDPG critic network for each of the 15 cases under the following conditions: The reward for each step that leads to a non-terminal state is -1 (to encourage fast solutions), the reward for reaching the terminal state is 0. The states were assigned 2D-coordinates as from the graph illustration (0: $[0, 0]$, 1: $[-1, 1]$, 2: $[1, 1]$) and the action to move from state s to state s' was defined as the offset $a = s' - s$. For the critic network we chose two layers with 4 hidden states, ReLU activations (except on the output) and Xavier-initialization. The policy was computed as in tabular Q-learning by selecting the action with highest Q-value for a given state. We performed ten thousand updates for each case consisting of all available transitions. The whole procedure was repeated with 10 random seeds (drawn uniformly from $[0, 1000]$).

Confirming the finding in Van Hasselt et al. (2018), no *unbounded* divergence occurred (which would cause floating point NaNs). However, we found occurrences of *soft* divergence (causing Q-values beyond the realizable range as given in Eq. (1)). In particular, we have computed the standard deviation of Q-values for each transition over the different random seeds. Evaluating the results (Figure 2) for the following four categories of transitions (s, a, r, s', t) reveals the relation between graph structure and soft divergence:

Transitions where s' is terminal are referred to as *directly connected*. Their Q-values are estimated almost perfectly, because Q-learning is reduced to supervised learning in these cases (cf Eq. (3)).

Transitions that end in a non-terminal state from which a terminal state is reachable are referred to as *connected*. Their Q-estimates exhibit only slightly more variance than the directly connected transitions. Presumably the reachable terminal state still acts as an anchor for the Q-value (as long as all transitions on the path are regularly used for updates). In line with this hypothesis, the two following categories that do not have an anchor show significantly more variance in their predictions:

If no terminal state is reachable from s' and there is no infinite path from s', the transition is referred to as a *loose end*. These transitions occur for instance at the end of each episode in episodic learning setups, when the agent is reset to a starting position. It is insightful to note that Q-values for such transitions are conceptually ill-defined in tabular Q-learning where a state without successors would be defined as terminal. For non-terminal states, a Q-value could be determined under the assumption that further transitions exist (and just have not been experienced yet), but then the Q-value is estimated using bootstrapping from another Q-value that has never been explicitly updated. This may be okay, if the function generalizes nicely from states with well-defined Q-values to loose ends – however there is no guarantee for this to happen.

Transitions are referred to as *disconnected* if no terminal state is reachable from s' but there exists at least one infinite path from s'. These transitions caused the highest variance in Q-estimates. In contrast to loose ends however, the Q-value for these transitions is well-defined under the assumption that all possible transitions are known (cf. Eq. (2)). The method we will introduce in the following builds on the insight that state of the art deep off-policy RL only updates their networks from a finite set of transitions; but for disconnected transitions the estimate suffers from high variance although exact Q-values can be computed under the assumption of complete replay memories. This even holds in our educational toy example in which no data was ever added or removed from the replay memory. Our method will compute the exact Q-values for a subproblem and use them for the original learning problem in the form of lower bounds. We will show empirically that, besides further effects, this reduces the variance of predicted Q-values.

5 METHOD

Despite the continuous state-action space, the networks in DDPG are updated based on a finite set of transitions from the replay memory. It is therefore possible to take a graph perspective on this data: A transition (s, a, r, s', t) can be seen as an edge between the nodes corresponding to states s and s' (which is terminal iff indicated by t); and can be annotated with r and a. We refer to this directed graph as *data graph* (see Figure 1 for an illustration).

QGRAPH

Building on the insights from section 4, we extract all transitions except for loose ends from the data graph. That is, we select the largest set of transitions from the *data graph* for which exact Q-values can be computed under the assumption that the resulting graph is complete (i.e. that all possible transitions and all states are included). This graph formally induces a smaller finite MDP for which the associated Q-function can be computed using tabular Q-iteration with guaranteed convergence due to its contraction property. We refer to this subgraph, annotated with exact Q-values for the simplified MDP, as QGRAPH.

The Q-values on the QGRAPH can be efficiently computed, e.g. by solving the linear equation system for a sparse transition matrix or a standard dynamic programming approach to Q-Iteration: For transitions to terminal states, the Q-value corresponds to the observed reward. Small transition loops are possible, for instance if an agent gets stuck at an obstacle, and are efficiently treated using Eq. (2). Whenever a Q-value is newly added or changed, the Q-values of all predecessors are updated recursively until no Q-values are changing anymore. Thus, the QGRAPH can easily be constructed incrementally as more data comes in and does not need to be built from a classic replay memory or data graph for each training.

In many settings, there are known *zero actions* a_z that do not change the agent's state at all, e.g. moving by 0 units or applying 0 force. If those are applicable in all states, it may be possible to add a self-loop to every single node in the data graph. This effectively eliminates all lose ends and turns them into disconnected states, in other words it enables the QGRAPH to contain all transitions from the data graph.

QGRAPH values as lower bounds on the original Q-learning problem

In most cases, the original MDP actually contains more states or transitions than the simplified MDP induced by the QGRAPH, in particular for all settings with continuous state-action spaces. Then, the Q-values do not transfer to the original MDP as a correct solution but in deterministic environments, they can serve as a lower bound for the true Q-values:

Each Q-value $\mathcal{Q}(s, a)$ on the QGRAPH is based on actually experienced trajectories, but it is possible that unseen states and transitions exist. Assume that transitions (s_0, a_1, r_1, s_1) and (s_1, a_2, r_2, s_2) are already known and part of the QGRAPH, but in fact at least one further transition from s_1 exists. Then the Q-value for the first transition is lower bounded by $\mathcal{Q}(s_1, a_2)$ because of the $\max$ operation:

$$\mathcal{Q}(s_0, a_1) = r + \max_a \mathcal{Q}(s_1, a) \geq r + \mathcal{Q}(s_1, a_2)$$

Thus, each Q-value for a transition in our QGRAPH is a lower bound of the Q-value for the same transition in the original MDP on continuous state and action spaces.

QGRAPH-bounded Q-learning

Q-values from our QGRAPH can be used as lower bounds in bootstrapping for temporal difference learning as in Eq. 3 – a method we call QGRAPH-*bounded Q-learning*:

$$\mathcal{Q}'(s, a) = \max(\text{LB}, r + \cdot\gamma \max_{a'} \mathcal{Q}(s', a')) \tag{4}$$

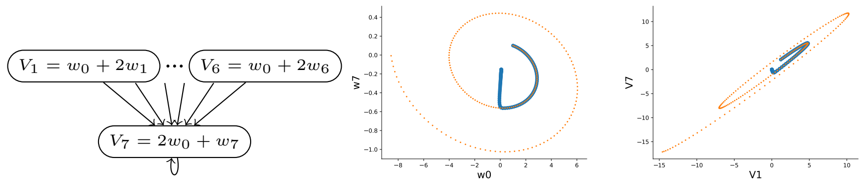

Figure 4: The 7-state star problem (Baird, 1999). Using vanilla TD-learning, state values and weights spiral out to infinity (orange dots). Applying our graph perspective however makes TD-learning converge to the correct solution (blue solid line).

where LB represents a per-sample lower bound.

Loose ends are not associated with such a lower bound but could potentially still carry important information (e.g. in cases where the function approximator has generalized nicely to the states involved). The transitions associated with loose can therefore still be used as usual, i.e. using unbounded TD-learning.

6 Experimental Results

We evaluated the core of our method on a classical toy example and empirically examine further aspects of the method on a simulated peg-in-hole problem.

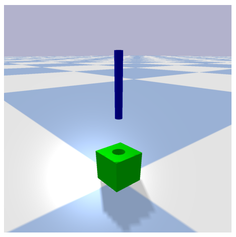

Figure 3: Simulated Peg-In-Hole task.

6.1 Baird's Star Problem

The 7-state star problem (Figure 4) was proposed by Baird (1999) to demonstrate convergence issues in value iteration with (linear) function approximation. The agent receives a reward of zero for each action and thus the correct solution to the problem is to set all weights to zero and obtain state-values of zero. If all weights are initially positive and w_0 larger than the others, this causes oscillatory behavior of both state values and weights. We reproduced the exact setting and result plots for Figure 4.2 in Baird (1999). Applying our graph view to the problem, we can derive a lower bound of zero for V_7 because it has a self-loop with reward 0; and thus this lower bound recursively leads to a lower bound of $0+\gamma V_7 = 0$ for all other states. These graph-based bounds can be applied in TD learning in analogy to Eq. (4) as $V'(s) = \max(LB, r + \gamma V(s'))$. As a result, our method converges to the correct state values rather than diverging to infinity as Figure 4 illustrates.

6.2 Experimental Setup

All further experiments were conducted in a simulated environment, see environment details in Appendix A.1 and DDPG implementation details in Appendix A.2. After each epoch, the Q-targets were updated, i.e. no explicit target network was used, since those are known to prolong training and thereby postpone convergence issues but not solve them (Van Hasselt et al., 2018). All algorithms were tested for 300 episodes. We tested vanilla DDPG on a grid of learning rates for actor and critic in $\{10^{-2}, 10^{-3}, 10^{-4}\}$ and chose three cases that are representative for the spectrum of DDPG performance. The learning curves for all learning rates are shown in Appendix 7. Most results will be presented in the form of learning curves, where the line represents the mean performance over ten runs with different random seeds and the shaded area highlights the standard deviation of the mean estimator, i.e. $\frac{\sigma}{\sqrt{n}}$.

6.3 Sample Efficiency and Robustness to Hyperparameters

We hypothesized that QGraph-based lower bounds would correctly limit the range of Q-values which prevents some cases of soft divergence and thereby increases sample efficiency. We further hypothesized that explicit bounds would barely have any impact in cases when vanilla Q-learning

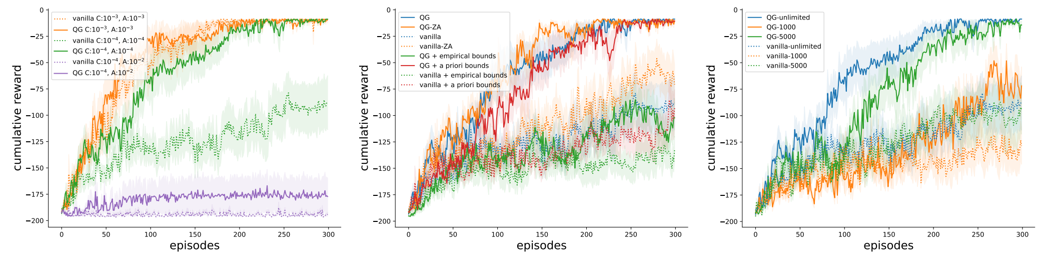

Figure 5: Learning curves for vanilla DDPG and QGRAPH-bounded Q-learning('QG') on the left; a number of baselines in the center; and performance under limited graph capacity on the right.

works well, because our method as described in Eq. (4) reduces to standard TD learning when no bound is violated. In other words this implies that QGRAPH-bounded Q-learning should never decrease performance.

For a first overview, we compared learning curves of QGRAPH-bounded Q-learning ('QG') to those of vanilla DDPG in Figure 5 (left). As expected, QGRAPHs speed up learning for all examined learning rates. The effect size varies and is larger for those learning rates that lead to relatively poor performance in vanilla DDPG. This decrease the gap in performance between different learning rates and can therefore be interpreted as an indicator for increased robustness to hyperparameters.

6.4 Variance of predictions

To assess if this performance is due to similar effects as in our educational examples, we evaluated the variance in predicted Q-values at the end of each experiment under the learning rate with largest effect size (10^{-4}). We covered the state space with a regular grid of 27 states and evaluated the learned Q-value for each of these states with a set of eleven given actions as well as with the action that the actor network suggests for each state. The full list of all states and given actions that were tested can be found in Appendix A.4.

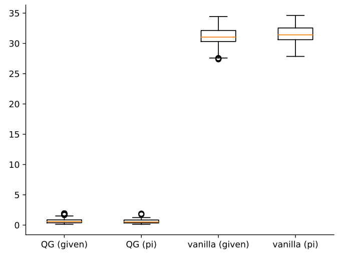

Figure 6: Standard deviation of predicted Q-values.

For the boxplot in Figure 6, we collected the standard deviations over the predicted Q-values for each state-action pair from 10 runs with different random seeds. The orange line indicates the median value, the box extends from the lower to the upper quartile value, the whiskers cover 1.5 times the inter quartile range and outliers are shown as circles. The results shows very clearly that QGRAPH-runs resulted in significantly less variance for predicted Q-values, indicating that QGRAPH-bounded Q-learning does indeed prevent cases of soft divergence.

6.5 Further Baselines

We ran the following baselines to deepen our understanding of the previously reported effects:

In many settings a *zero action* is known that does not change the agent's state (in our case it is the offset in position by zero meters). Adding hypothetical transitions with the zero action after each physical transition ('vanilla-ZA') improves the structure of the data graph by turning loose ends into disconnected transitions. Using zero actions in our method ('QG-ZA') not only improves the structure of the data graph but also spreads information in the form of lower bounds to predecessors in the QGRAPH. The results in the center of Figure 5 show that zero actions improve marginally over vanilla DDPG and QGRAPH-bounded Q-learning. This implicates on the one hand that the structure of the data graph matters and that in particular vanilla DDPG benefits from a structure without loose ends. A the same time, adding our QGRAPHis much more effective than changing the data graph only. This demonstrates that the propagation of information through the QGRAPH and the integration of lower bounds into TD-learning are the main contribution of our method.

The next set of baselines was designed to evaluate how much influence the exact bounds have. Bounded temporal difference learning could, besides our QGRAPH-based bounds, integrate two further types of lower and upper bounds: *A priori* bounds may be known in the case of a bounded reward function, see Eq. (1). *Empirical* bounds may seem like an alternative for correct a priori bounds: rather than using known bounds on the reward, these bounds could be estimated from experience. Note that the true Q-values are guaranteed to lie within QGRAPH-based bounds and correct a priori bounds, while empirical bounds might be too tight. We combined QGRAPH-bounded Q-learning and vanilla DDPG with both types of bounds. When several bounds were available for one Q-value, the tightest upper and lower bound were chosen. The results in Figure 5 confirm that incorrect empirical bounds (green lines) have adverse effects on both methods, while a priori bounds do not seem to have any significant effect. We conclude that the tight sample-specific lower bounds from our QGRAPH are key and much more informative than more general bounds.

6.6 LIMITED GRAPH CAPACITY

In deep reinforcement learning, the replay memory is typically a FIFO-buffer, i.e. those elements that were added first are overwritten first when the buffer is full ('first in, first out'). For a data graph, it is possible to delete single transitions but there are two possible effects: On the one hand, some information from deleted transitions can be implicitly contained in its predecessors' Q-values on the QGRAPH, which could imply that our method is more robust to small memory capacities. On the other hand, cuts from deleted transitions can stop information propagation through the QGRAPH, which could in turn slow down further progress. We therefore empirically compared the drop in performance for vanilla DDPG and our QGRAPH-bounded Q-learning with graph capacities of 1000 and 5000 transitions. For comparison, the average unlimited graph contained roughly 30,000 unique transitions at the end of our 300 episode experiments. As the right plot in Figure 5 illustrates, a QGRAPH-based method that is limited to only 1000 samples still performs on par with unlimited vanilla DDPG, while the vanilla DDPG performance decreases for a limit of 1000 transitions. Higher graph capacities do not seem to impact performance significantly.

7 CONCLUSION

From the observation that even for continuous state and action spaces, model-free off-policy deep reinforcement learning algorithms perform network updates on a finite set of transitions, we have developed a graph perspective on the replay memory that allows closer analysis. Exploiting the graph structure, we chose a subset of transitions that give rise to a simplified MDP for which exact Q-values can be computed. We have shown that these Q-values can serve as lower bounds for the actual Q-learning problem on the full state-action space.

Our method converges on Baird's classical star problem and empirically enhances DDPG performance on a simulated peg-in-hole task. The largest boost in performance was observed for those hyperparameters that lead to worst DDPG performance, supporting the view that our method prevents some degenerate cases in function approximation for model-free off-policy deep reinforcement learning. Additionally, the QGRAPH that holds the lower bounds, provides an additional kind of memory for information from transitions which have already been overwritten in the replay memory.

The current version of this method is only guaranteed to be correct in deterministic environments, leaving a probabilistic extension for future work. Furthermore, we believe that the reward function interacts with soft divergence in Q-learning and might examine potential implications for reward shaping in the future.

REFERENCES

Artemij Amiranashvili, Alexey Dosovitskiy, Vladlen Koltun, and Thomas Brox. Td or not td: Analyzing the role of temporal differencing in deep reinforcement learning. In *International Conference on Learning Representations (ICLR)*, 2018.

Leemon Baird. Residual algorithms: Reinforcement learning with function approximation. In *Machine Learning Proceedings 1995*, pp. 30–37. Elsevier, 1995.

Leemon C Baird. Reinforcement learning through gradient descent. *PhD thesis, Carnegie Mellon University*, 1999. URL http://reports-archive.adm.cs.cmu.edu/anon/1999/CMU-CS-99-132.pdf.

Andreas Doerr, Michael Volpp, Marc Toussaint, Trimpe Sebastian, and Christian Daniel. Trajectory-based off-policy deep reinforcement learning. In *International Conference on Machine Learning*, pp. 1636–1645, 2019.

Honghua Dong, Jiayuan Mao, Xinyue Cui, and Lihong Li. Explicit recall for efficient exploration, 2019. URL https://openreview.net/forum?id=B1GIB3A9YX.

Gregory Farquhar, Tim Rocktaeschel, Maximilian Igl, and Shimon Whiteson. TreeQN and ATreec: Differentiable tree planning for deep reinforcement learning. In *International Conference on Learning Representations*, 2018. URL https://openreview.net/forum?id=H1dh6Ax0Z.

Nima Fazeli, Samuel Zapolsky, Evan Drumwright, and Alberto Rodriguez. Learning data-efficient rigid-body contact models: Case study of planar impact. In *Conference on Robot Learning*, pp. 388–397, 2017.

Kaiming He, Xiangyu Zhang, Shaoqing Ren, and Jian Sun. Delving deep into rectifiers: Surpassing human-level performance on imagenet classification. In *Proceedings of the IEEE international conference on computer vision*, pp. 1026–1034, 2015.

Peter Henderson, Riashat Islam, Philip Bachman, Joelle Pineau, Doina Precup, and David Meger. Deep reinforcement learning that matters. In *Thirty-Second AAAI Conference on Artificial Intelligence*, 2018.

Kanghoon Lee and Kee-Eung Kim. Tighter value function bounds for bayesian reinforcement learning. In *Twenty-Ninth AAAI Conference on Artificial Intelligence*, 2015.

Sergey Levine, Peter Pastor, Alex Krizhevsky, and Deirdre Quillen. Learning hand-eye coordination for robotic grasping with deep learning and large-scale data collection. *CoRR*, abs/1603.02199, 2016.

Timothy P Lillicrap, Jonathan J Hunt, Alexander Pritzel, Nicolas Heess, Tom Erez, Yuval Tassa, David Silver, and Daan Wierstra. Continuous control with deep reinforcement learning. *arXiv preprint arXiv:1509.02971*, 2015.

Hamid Reza Maei, Csaba Szepesvári, Shalabh Bhatnagar, Doina Precup, David Silver, and Richard S. Sutton. Convergent temporal-difference learning with arbitrary smooth function approximation. In *NIPS*, 2009.

Hamid Reza Maei, Csaba Szepesvári, Shalabh Bhatnagar, and Richard S Sutton. Toward off-policy learning control with function approximation. In *ICML*, pp. 719–726, 2010.

Horia Mania, Aurelia Guy, and Benjamin Recht. Simple random search of static linear policies is competitive for reinforcement learning. In *Advances in Neural Information Processing Systems*, pp. 1800–1809, 2018.

Volodymyr Mnih, Koray Kavukcuoglu, David Silver, Andrei A Rusu, Joel Veness, Marc G Bellemare, Alex Graves, Martin Riedmiller, Andreas K Fidjeland, Georg Ostrovski, et al. Human-level control through deep reinforcement learning. *Nature*, 518(7540):529, 2015.

Volodymyr Mnih, Adria Puigdomenech Badia, Mehdi Mirza, Alex Graves, Timothy Lillicrap, Tim Harley, David Silver, and Koray Kavukcuoglu. Asynchronous methods for deep reinforcement learning. In *International Conference on Machine Learning*, pp. 1928–1937, 2016.

Rémi Munos, Tom Stepleton, Anna Harutyunyan, and Marc Bellemare. Safe and efficient off-policy reinforcement learning. In *Advances in Neural Information Processing Systems*, pp. 1054–1062, 2016.

Harm van Seijen, Shimon Whiteson, Hado van Hasselt, and Marco Wiering. Exploiting best-match equations for efficient reinforcement learning. *Journal of Machine Learning Research*, 12(Jun): 2045–2094, 2011.

A Shkolnik and R Tedrake. Path planning in 1000+ dimensions using a task-space voronoi bias. *Robotics and Automation*, pp. 2061–2067, 2009.

David Silver, Julian Schrittwieser, Karen Simonyan, Ioannis Antonoglou, Aja Huang, Arthur Guez, Thomas Hubert, Lucas Baker, Matthew Lai, Adrian Bolton, et al. Mastering the game of go without human knowledge. *Nature*, 550(7676):354, 2017.

Richard S Sutton and Andrew G Barto. *Reinforcement learning: An introduction*. MIT press, 2018.

Hado Van Hasselt, Yotam Doron, Florian Strub, Matteo Hessel, Nicolas Sonnerat, and Joseph Modayil. Deep reinforcement learning and the deadly triad. *arXiv preprint arXiv:1812.02648*, 2018.

A Appendix

A.1 Peg-In-Hole Environment Details

The environment was implemented using pybullet[1] A blue peg is supposed to be inserted into a green object (see Figure 3). The peg is always upright and velocity-controlled: an action represents the three-dimensional offset to the next position. The simulation is stepped forward until a stable new position is reached. The actions are box-constrained to $[-1, 1]$ in each dimension which corresponds to a movement of 1cm. The green object has a width of 5cm and is within a cubic state space of width 20cm. The peg has a diameter of 1cm, the hole's diameter is 2cm. The agent receives a distance-based reward $r = \exp(-\frac{\delta}{0.03}) - 1$, where δ is the Euclidean distance to the goal position in meters.

A.2 Network Details

The critic network consists of three fully connected layers with 200 nodes each. For the inner layers, ReLU activations were used. The network was initialized with weights sampled from a normal distribution of mean 0 and std 0.001. The actor network also consists of three fully connected layers with 200 nodes each, but used tanh activations and was initialized from a He-uniform distributions (He et al., 2015).

All neural networks were implemented using tensorflow[2] and optimized using the AdamOptimizer, with 50 training epochs after each episode (i.e. 200 agent steps) and up to 15 random mini batches of data per epoch.

A.3 Detailed Performance for Different Learning Rates

We ran vanilla DDPG on a grid of learning rates where both actor and critic learning rates is chosen from $\{10^{-2}, 10^{-3}, 10^{-4}\}$. We chose the three curves with solid lines as representative for the spectrum of performance and based all further evaluation on these learning rates.

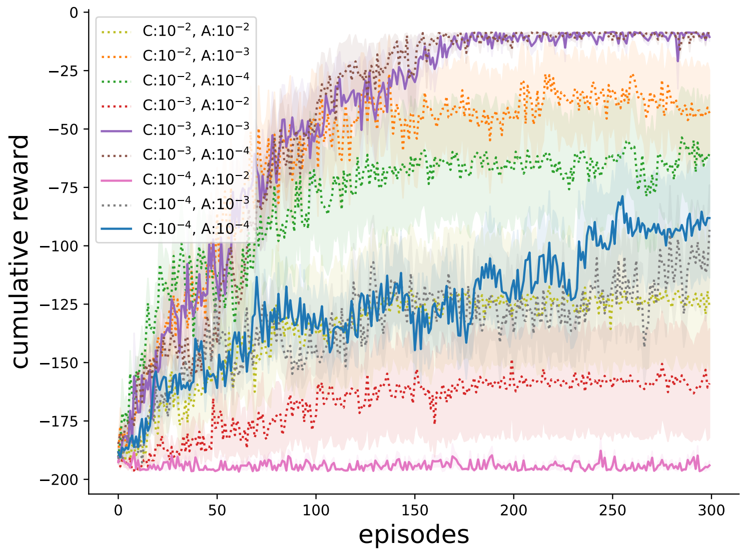

Figure 7: Vanilla DDPG performance for all tested learning rates.

[1]`https://github.com/bulletphysics/bullet3`
[2]`www.tensorflow.org`

A.4 State-Action pairs tested for variance in predicted Q-values

Here we show all states and actions that were used to examine the variance in Q-estimates in Figure 6.

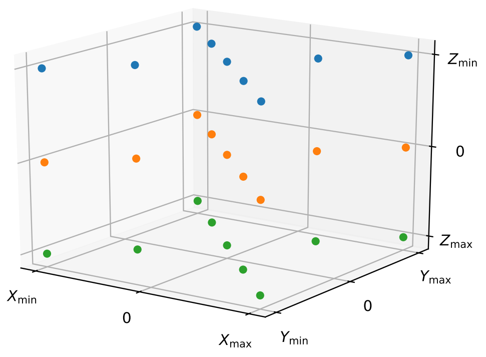

a_x	a_y	a_z
0	0	0
0	0	1
0	0	-1
0	1	0
0	-1	0
1	0	0
-1	0	0
0.5	0.5	0.5
-0.5	-0.5	-0.5
1	1	1
-1	-1	-1